

# Supporting Information

## Electrochemically Controlled RAFT Polymerization for Highly Sensitive

### Electrochemical Biosensing of Protein Kinase Activity

Qiong Hu,<sup>‡,§,†</sup> Jinming Kong,<sup>\*,‡</sup> Dongxue Han,<sup>§,†</sup> Yuwei Zhang,<sup>\*,§</sup> Yu Bao,<sup>§</sup> Xueji Zhang,<sup>‡</sup> and Li Niu<sup>\*,§,†</sup>

<sup>‡</sup> *School of Environmental and Biological Engineering, Nanjing University of Science and Technology, Nanjing 210094, P. R. China.*

<sup>§</sup> *Center for Advanced Analytical Science, % School of Chemistry and Chemical Engineering, % MOE Key Laboratory for Water Quality and Conservation of the Pearl River Delta, Guangzhou University, Guangzhou 510006, P. R. China.*

<sup>†</sup> *School of Civil Engineering, Guangzhou University, Guangzhou 510006, P. R. China.*

\*E-mail: [j.kong@njust.edu.cn](mailto:j.kong@njust.edu.cn). Tel.: +86-25-84303109.

\*E-mail: [ccywzhang@gzhu.edu.cn](mailto:ccywzhang@gzhu.edu.cn). Tel.: +86-020-39366902.

\*E-mail: [lniu@gzhu.edu.cn](mailto:lniu@gzhu.edu.cn). Tel.: +86-020-39366902.

#### Table of contents:

**Figure S-1:** Surface coverage of substrate peptide and MCH.

**Figure S-2:** Effect of MCH on charge transfer.

**Figure S-3:** Elemental mapping of the AuE/S<sub>p</sub>/MCH/Zr<sup>4+</sup>/CPAD/Fc.

**Figure S-4:** Optimization of BrPhN<sub>2</sub><sup>+</sup> concentration.

**Table S-1:** Values of  $R_{ct}$ ,  $CPE$ ,  $R_s$ , and  $W$  of differently modified electrodes.

**Table S-2:** Comparison of the analytical performance with those of other methods.

**Table S-3:** Detection of PKA activity in serum samples.

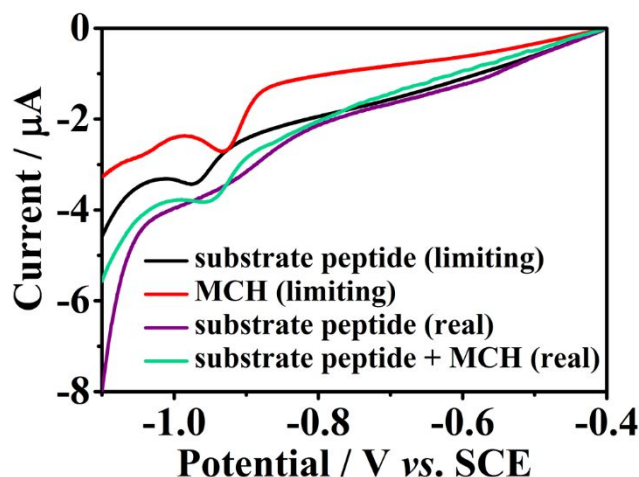


**Figure S-1:** LSV curves of differently modified electrodes. Scan rate:  $20 \text{ mV s}^{-1}$ ; quiet time: 1.0 min. “limiting” represents the maximal surface coverage of substrate peptide or MCH, “real” represents the real surface coverage of substrate peptide or substrate peptide/MCH of the gold electrode modified as described in the Experimental Section. Surface coverage ( $\Gamma_m$ ) can be calculated according to  $\Gamma_m = Q_m/FAv$ , where  $Q_m$ ,  $F$ ,  $A$  and  $v$  represent the integral value of the reductive desorption wave (A V), the Faraday constant ( $96485.33 \text{ C mol}^{-1}$ ), the electrochemical surface area ( $0.07 \text{ cm}^2$ ), and the scan rate ( $0.02 \text{ V s}^{-1}$ ). The  $\Gamma_m$  values of substrate peptide (limiting), MCH (limiting), substrate peptide (real), and substrate peptide + MCH (real) are calculated to be  $2.10 \times 10^{-10} \text{ mol cm}^{-2}$ ,  $3.84 \times 10^{-10} \text{ mol cm}^{-2}$ ,  $1.30 \times 10^{-10} \text{ mol cm}^{-2}$ , and  $2.64 \times 10^{-10} \text{ mol cm}^{-2}$ , respectively. Assuming that the surface areas occupied by a substrate peptide or a MCH molecule is  $a$  and  $b$  respectively, then  $2.10a = 3.84b$ . As calculated, the surface area occupied by the substrate peptide + MCH (real) is  $3.72b$ . Thus,  $\sim 96.9\%$  (i.e.,  $3.72b/3.84b$ ) of the electrode surface is occupied by the substrate peptide and MCH (real).

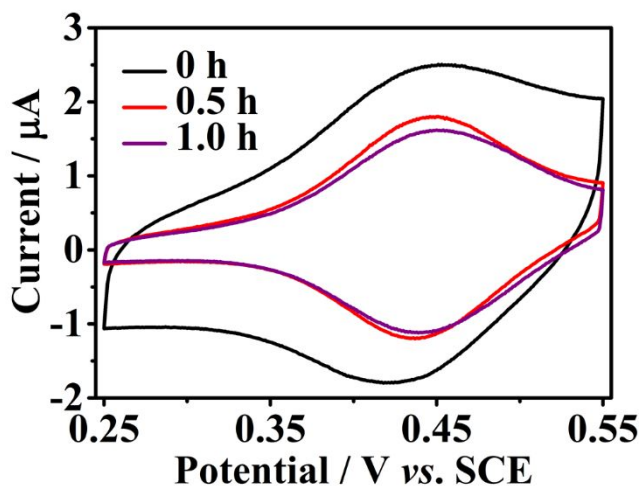


**Figure S-2:** Effect of MCH blocking time on the charge transfer of the Fc-SLGGGGC-modified gold electrode. Fc-SLGGGGC:  $1.0 \text{ }\mu\text{M}$ ; modification time: 1.0 h; MCH:  $2.0 \text{ mM}$ ; supporting electrolyte:  $0.5 \text{ M LiClO}_4$ ; scan rate:  $0.1 \text{ V s}^{-1}$ ; quiet time: 30 s. The blocking of the electrode surface leads to a decrease of the

oxidation peak current by 1.04% (0.5 h) and 7.8% (1.0 h), respectively. The small decrease in oxidation peak current may be ascribed to the substitution of some of the pre-immobilized Fc-modified peptides by MCH molecules during the MCH blocking. With this in mind, the blocking of the electrode surface with MCH has little effect on the charge transfer between the surface-tethered Fc tags and the electrode surface.

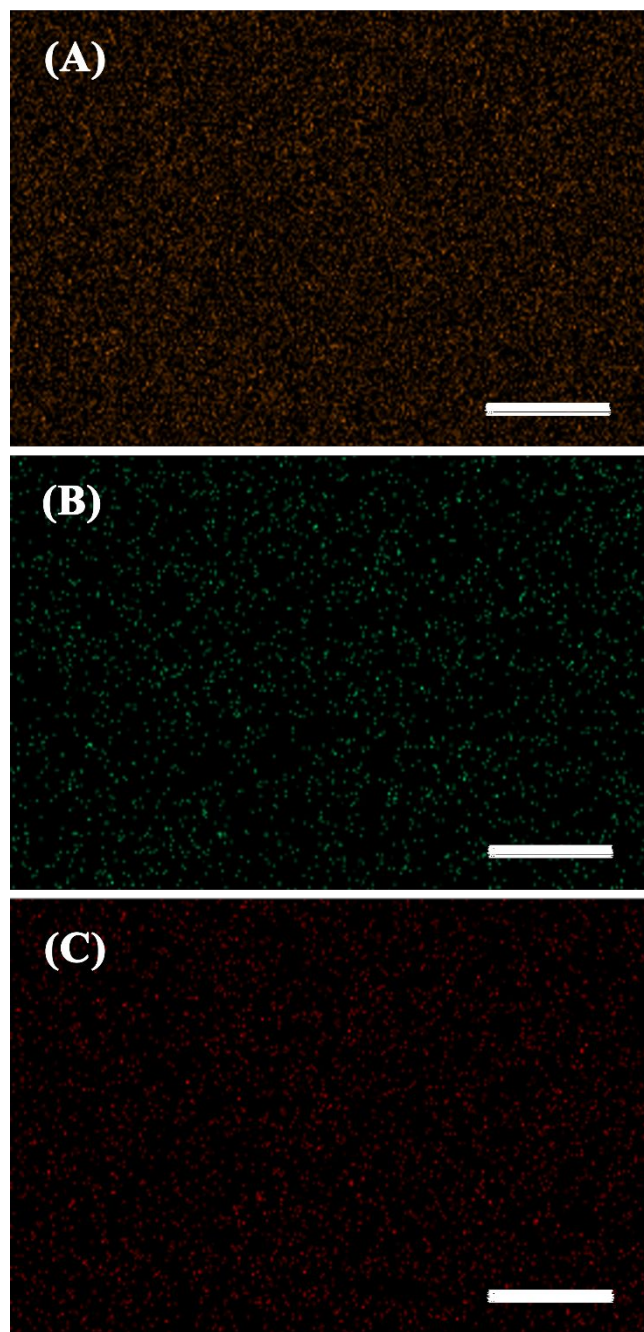


**Figure S-3:** The traces of P element (A), Br element (B), and Fe element (C). The scale bar is 1.0  $\mu\text{m}$ .

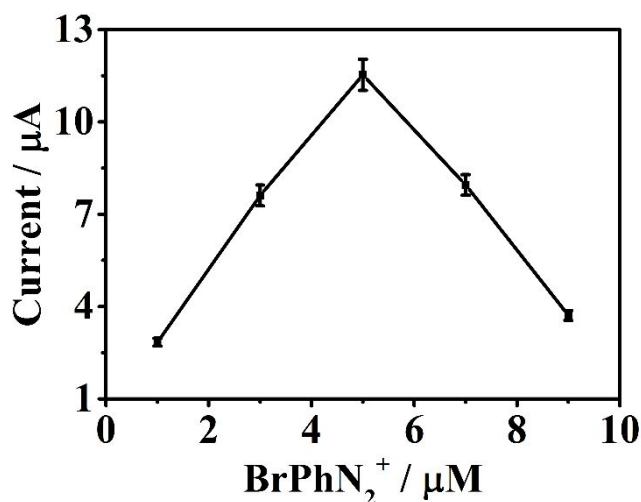


**Figure S-4:** Oxidation currents at  $\sim 0.3$  V in the presence of different concentrations of BrPhN<sub>2</sub><sup>+</sup>. PKA, 140 mU mL<sup>-1</sup>. Error bars show the SDs of five independent assays.

**Table S-1:** Values of  $R_{ct}$ ,  $CPE$ ,  $R_s$ , and  $W$  of Differently Modified Electrodes

Electrode	$R_{ct}$ ( $\Omega$ )	$CPE$ ( $\times 10^{-6}$ S sec <sup>n</sup> )	$R_s$ ( $\Omega$ )	$W$ ( $\times 10^{-4}$ S sec <sup>0.5</sup> )
AuE	$\sim 143.7$	$\sim 1.41$	$\sim 152.9$	$\sim 7.74$
AuE/S	$\sim 772.5$	$\sim 1.37$	$\sim 162.3$	$\sim 7.26$
AuE/S/MCH	$\sim 1891$	$\sim 0.81$	$\sim 168.9$	$\sim 7.06$
AuE/S <sub>p</sub> /MCH	$\sim 2117$	$\sim 1.16$	$\sim 157.2$	$\sim 6.96$
AuE/S <sub>p</sub> /MCH/Zr <sup>4+</sup>	$\sim 2568$	$\sim 1.05$	$\sim 156.9$	$\sim 6.95$
AuE/S <sub>p</sub> /MCH/Zr <sup>4+</sup> /CPAD	$\sim 2756$	$\sim 1.12$	$\sim 143.6$	$\sim 6.80$
AuE/S <sub>p</sub> /MCH/Zr <sup>4+</sup> /CPAD/Fc	$\sim 648.2$	$\sim 1.43$	$\sim 157.9$	$\sim 7.54$

**Table S-2:** Comparison of the Analytical Performance with Those of Other Methods

Method	Amplification	Linear range* (U mL <sup>-1</sup> )	LOD (mU mL <sup>-1</sup> )	Mode	Ref.
Electrochemical	DNA-AuNPs	0.03–40	30	Signal-on	6
Electrochemical	eATRP	0–0.14	1.63	Signal-on	8
Fluorometric	CdSe/ZnS QDs@SiO <sub>2</sub> NPs	0.01–40	4.0	Signal-on	9
Fluorometric	Metal nanoclusters	0.4–3.0	100	Signal-on	10
Fluorometric	Gold nanoclusters	0.01–40	4.0	Signal-on	11
PEC	ALP	0.05–100	170	Signal-on	15
ECL	AuNPs	0.01–10	5.0	Signal-on	17
Electrochemical	TiO <sub>2</sub> NPs	0–1.0	200	Signal-on	18
Electrochemical	RCA	5.0–500	500	Signal-on	29
Electrochemical	eRAFT polymerization	0–0.14	1.02	Signal-on	This work

\*The normal range of extracellular PKA activity in the serum of healthy individuals is 0–10.6 mU mL<sup>-1</sup>.

**Table S-3:** Detection of PKA Activity in Serum Samples

Samples	Commercial ELISA kit			The as-fabricated biosensor	
	PKA spiked (mU mL <sup>-1</sup> )	PKA detected (mU mL <sup>-1</sup> )	Recovery (%)	PKA detected (mU mL <sup>-1</sup> )	Recovery (%)
1	0	4.47			
2	70	72.65	97.56	73.02	98.05
3	140	147.53	102.12	148.16	102.55